Superconducting vortex with extended core

Herman J. Fink
Department of Electrical Engineering and Computer Science, University of California–Davis, Davis, California 95616
(Received 27 September 1991)

A bridge-type superconducting microcircuit in a magnetic field was analyzed using the nonlinear Ginzburg-Landau theory. There exist two different spatial configurations of the order parameter; one has a maximum in the central branch and minima in the current-carrying branches, while the other is a vortex with zero order parameter over part of the central branch. For higher temperatures, near the second-order phase-transition boundary, the vortex has a point singularity, while at lower temperatures it has an *extended* core, a notable feature in superconductivity. The phase transition between the two vortex states is first order.

Future implementation of superconducting microcircuitry will require fundamental understanding of currents in micronets where the distances between the nodes are of the order of magnitude of the temperature-dependent coherence length $\xi(T)$. With that in mind we investigate a bridge-type circuit, consisting of two unit cells of equal area and three branches of equal length, shown in the inset (a) of Fig. 1 [bridge], with respect to the phase-transition boundaries, the magnetic properties in terms of persistent currents, and the Gibbs free energy.

The starting point of this work is the one-dimensional, nonlinear Ginzburg-Landau (GL) equations. Assuming constant wire cross section and replacing the gauge-invariant superfluid velocity by the normalized current density J, we obtain, after integrating once, the following equation:[1]

$$2f^2(df/dx)^2 = (f_0^2-f^2)[f^2(2-f_0^2-f^2)-2J^2/f_0^2] , \quad (1)$$

where x is the curvilinear coordinate along a branch, normalized by $\xi(T)$. The normalized complex order parameter $\Psi(x)=f(x)\exp[i\theta(x)]$. Its modulus is $f(x)$ [modulus of the order parameter (MOP)] and f_0 is the value of $f(x)$ at an extremum. Equation (1) is valid for temperatures at or below the second-order phase-transition (SOPT) boundary $T_c(\phi)$, shown in Fig. 1 by the lower solid curve. For fixed R and $\xi(0)$, the ordinate $R/\xi(T)$ in Fig. 1 is a function on temperature T. The equations describing these curves are obtained from the linearized GL equations with $J=0$ by applying the nodal conditions of Ref. 2 which assume without physical justification that the algebraic sum of the derivatives of df/dx is zero at a node and $f(x)$ is continuous. In Ref. 3 the nodal conditions were explained by introducing the concept of complex current conservation and in Ref. 4 the generalized Kirchhoff current law (KCL) was introduced as a fundamental condition in terms of the conservation of the complex momentum density at a node. This led to the following nodal conditions:

$$\sum_\alpha J_\alpha = 0$$

and

$$\sum_\alpha df_\alpha^2/dx = 0 .$$

The first relation is KCL applicable to ordinary circuits, while the second is the same as stated in Ref. 2, provided that $f_\alpha \neq 0$ at the node (α signifies the branches connected to the node). If, however, $f_\alpha = 0$ at a node, then the difference between the nodal conditions of Refs. 2 and 4 becomes of significance as will be apparent below. The SOPT boundary obtained from the linearized GL equation is[3,5]

$$\pm 3\cos(\pi R/\xi) = 2\cos\gamma + 1 , \quad (2)$$

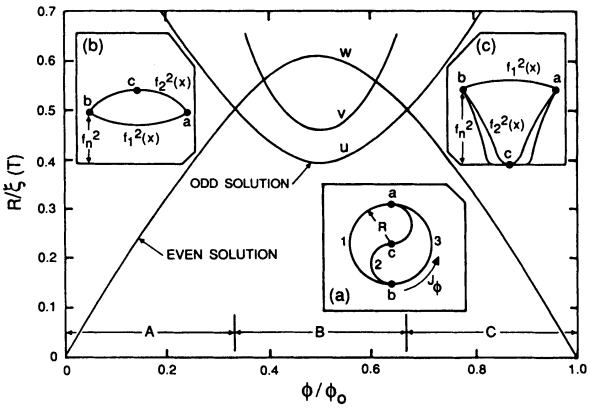

FIG. 1. The phase-transition boundaries of the bridge circuit which is depicted in inset (a). The region below the lower lines is the normal state. Curves u and w are second-order phase-transition boundaries. Curve v is a first-order phase-transition boundary separating a conventional vortex from one with an extended core. Note that $R/\xi(T) \propto (T_c - T)^{1/2}$, where T_c is the transition temperature at $\phi=0$. Insets (b) and (c) depict schematically $f^2(x)$ of the even and odd (vortex) solutions, along the various branches of the circuit.

 ©1992 The American Physical Society

where $\gamma=2\pi\phi/\phi_0$, and ϕ is the flux *per unit cell*. Equation (2) is compatible with a vector potential $\mathbf{A}=Br\hat{\varphi}/2$, where B is the magnetic flux density and $\hat{\varphi}$ is a unit vector in cylindrical coordinates (r,φ,z).

Although $f(x)\to 0$ at the SOPT boundary, one can use the solution of the linearized equation to predict certain features for $T<T_c(\phi)$. They are a guide in the search for nonlinear solutions and useful in checking the consistency of the linear and nonlinear results when $f(x)\ll 1$. These features are, assuming that $f(x)\ll 1$ but not zero,[5] the following.

(i) Along branch 2, the MOP in flux regions A $(0<\phi/\phi_0<\frac{1}{3})$ and C $(\frac{2}{3}<\phi/\phi_0<1)$, shown in Fig. 1, is

$$f_2(x)=f_a\cos(\tfrac{1}{2}\pi R/\xi-x/\xi)/\cos(\tfrac{1}{2}\pi R/\xi)\ , \tag{3}$$

and in flux region B $(\frac{1}{3}<\phi/\phi_0<\frac{2}{3})$ it is, for the smallest values of $R/\xi(T)$ (highest temperatures),

$$f_2(x)=f_a\sin(\tfrac{1}{2}\pi R/\xi-x/\xi)/\sin(\tfrac{1}{2}\pi R/\xi)\ . \tag{4}$$

The value of x is measured from node a. Equation (4) indicates that $f_2(x)$ is zero in the middle of branch 2, while in flux regions A and C it is maximum.

(ii) Consistent with the nodal conditions, branches 1 and 3 have nonzero minima of $f(x)$ halfway between nodes a and b in flux regions A and C, and maxima in flux region B.

(iii) In flux region B the curve denoted by u in Fig. 1 is the highest-temperature SOPT boundary.

(iv) Assume that $\Psi_a=f_a\exp(i\alpha)$ and $\Psi_b=f_b\exp(i\beta)$, and $f_a=f_b$ because of symmetry. One finds then from the nodal equations that

$$\exp[i(\beta-\alpha)]=3\cos(\pi R/\xi)/(2\cos\gamma+1).$$

Because of single valuedness of $\Psi(x)$, the phase difference $(\alpha-\beta)$ along all three branches much be the same within $2\pi n$, where n is an integer or zero. In flux region A it is 0 [positive sign in Eq. (2)], in B it is $\pm\pi$ [negative sign in Eq. (2)], and in C it is $\pm 2\pi$ for branches 1 and 3. For branch 2, $(\alpha-\beta)$ is zero in flux regions A and C since branch 2 does not carry a current and $f_2(x)$ at point c is maximum. If flux region B branch 2 does not carry a current either but $f_2(x)$ at point c is zero, thus breaking the continuity of the phase of $\Psi_2(x)$ at this point. Therefore, the phase θ_2 of $\Psi_2(x)$ must change discontinuously by $\pm\pi$ at the point at which $|\Psi_2(x)|=0$, consistent with the line integral taken over the second GL equation:

$$\Delta\theta_2=\frac{2\pi}{\phi_0}\int_a^b\frac{\mathbf{J}\cdot d\mathbf{x}}{f_2^2(x)}-\frac{2\pi}{\phi_0}\int_a^b\mathbf{A}\cdot d\mathbf{x}\ . \tag{5}$$

One can show that the line integral of the vector potential taken over branch 2 is zero. Therefore, the remaining line integral must be $\pm\phi_0/2$ due to the singularity of $f_2(x)$ at point c, giving rise to a phase flip center.[6]

We proceed now to the nonlinear calculations and results. Insets (b) and (c) of Fig. 1 show schematically the MOP on the various branches of the bridge resulting from computations of the even and odd (vortex) solutions, respectively. When Eq. (1) is solved numerically with the usual nodal conditions, we obtain the persistent current density $J_\phi\equiv J$ as a function of the extremal and nodal MOP's. Figure 2 shows J_ϕ as a function of f_{01}, f_n, and f_{02} for $R/\xi=0.45$ for (a) flux region A and (b) flux region B. In Fig. 2(a) the values of f_{01} and f_{02} are the extrema of $f(x)$ in branches 1 (the same as in branch 3) and 2, respectively, and f_n is $f(x)$ at nodes a and b. In Fig. 2b, f_{01} and f_n have the same meaning. the value of $f_{02}=0$ is $f_2(x)$ in the center of branch 2 in flux region B. $f_2(x)$ extends from f_{02} to f_n and extrapolates to a maximum value f'_{02} outside the type-I circuit. Equation (1) does not permit a solution of $f_2(x)$ larger than unity for $J=0$, even if extrapolated. When ϕ is varied for $R/\xi=0.45$, the bridge circuit goes from a strongly superconducting region $[f(x)=1]$ at $\phi=0$ to a SOPT boundary $[f(x)=0]$ at $\phi/\phi_0\approx 0.293$, then remains in the normal state until $\phi/\phi_0\approx 0.381$, enters the superconducting state at another SOPT boundary $[f(x)=0]$ and remains strongly superconducting $[f_{01}\approx 0.535]$ when $\phi/\phi_0\to\frac{1}{2}$.

After calculating $f(x)$ for a fixed J value, satisfying simultaneously the nodal conditions, we calculate the corresponding magnetic flux, linking the circuit, by taking a contour integration of the second GL equation. This yields [ϕ is the flux per unit cell, n is the phase twist number, and $f_3^2(x)=f_1^2(x)$]

$$2\pi\left[\frac{2\phi}{\phi_0}-n\right]=\oint\frac{\mathbf{J}_\phi\cdot d\mathbf{x}}{f_1^2(x)}\ . \tag{6}$$

Figure 2(c) shows J_ϕ (dimensionless) as a function of ϕ. The current density in conventional cgs Gaussian units is $J_{\rm conv}=J_\phi(c/4\pi)[\phi_0/(2\pi\xi\lambda^2)]$ statampere/cm^2. As ϕ is increased from zero to $\phi_0/2$, J_ϕ increases from zero, reaches a maximum, becomes zero at the SOPT boundary, and remains zero until the second SOPT boundary is

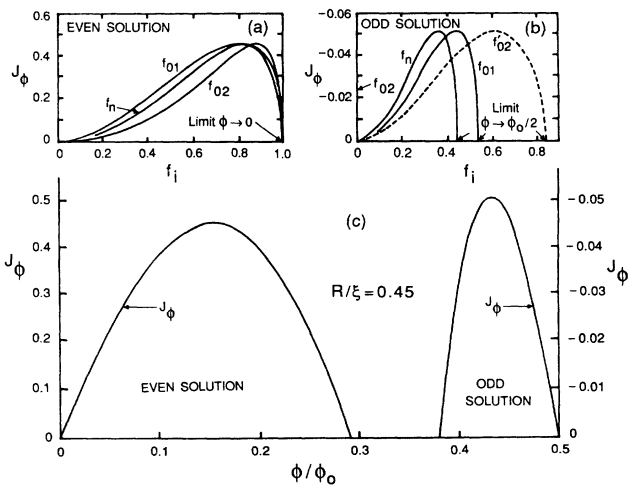

FIG. 2. Normalized persistent current density J_ϕ as a function of the moduli of the extremal and nodal order parameters on the various branches, for $R/\xi(T)=0.45$: (a) for flux region A of Fig. 1; (b) for flux region B of Fig. 1; (c) shows the corresponding J_ϕ as a function of magnetic flux ϕ, obtained from Eq. (6).

reached. Then it reverses direction, reaches a minimum and becomes zero at $\phi_0/2$. When $\phi > \phi_0/2$, the current reverses direction as ϕ is increased through $\phi_0/2$. J_ϕ has point symmetry around $\phi/\phi_0 = \frac{1}{2}$, $J_\phi = 0$.

It follows from Eq. (1) that

$$df_2/dx = [1-(1-f_{02}'^2)^2]^{1/2}/\sqrt{2}$$

in the center of branch 2 for the vortex solution. The value f_{02}' is the maximum of the $f_2(x)$ function on the extrapolated branch outside the bridge circuit. When R/ξ is increased at constant ϕ/ϕ_0, for example, f_{02}' increases also and reaches a maximum value very close to unity. When this occurs, the relation between R/ξ and ϕ/ϕ_0 is circumscribed by curve v in Fig. 1. For R/ξ and ϕ/ϕ_0 above this curve it is impossible to find a solution of the GL equation which satisfies the nodal conditions with $f_2(x)$ being zero only in the middle of branch 2. We call this spatial arrangement of $f_2(x)$ a conventional vortex. The normal state, $f(x)=0$, is also a possible solution of the GL equations in that region. However, this would imply a discontinuity in the Gibbs free energy, which is unreasonable. One can overcome this dilemna if we permit an enlarged normal region in the center of branch 2. This, one expects, would be a lower energy state than the normal state and make the energy continuous as one decreases the temperature at constant magnetic flux, for example. However, in that case another difficulty arises. The point where the extended normal core region $[f_2(x)=0]$ joins the superconducting region $[f_2(x)\neq 0]$ has to be treated as a node. If one takes the nodal conditions of Ref. 2 at face value, one finds that the algebraic sum of df_2/dx is not zero at this node since $f_2(x)$ is a Jacobian elliptic function which has a nonzero slope at a point where $f_2(x)=0$.

It has been shown recently[4] and mentioned above that one of the fundamental nodal conditions in micronetworks is the conservation of the complex momentum density at a node. In our case this reduces to $\sum[df_2^2(x)/dx_2]=0$. This nodal condition is satisfied at the point where the extended vortex core joins the $f_2^2(x)$ function and, therefore, justifies the extended vortex core solution.

Figure 3 shows J_ϕ as a function of ϕ for $R/\xi = 0.5$. Also shown are the MOP's for $\frac{1}{3} \le \phi/\phi_0 \le 0.5$. For $\phi/\phi_0 < \frac{1}{3}$ the solution is of the type shown schematically in Fig. 1(b). For $\frac{1}{3} \le \phi/\phi_0 < 0.428$ it is a conventional vortex, and for $0.428 < \phi/\phi_0 \le 0.5$ it is a vortex with an extended core with $f_{02}' \approx 0.997$ for the lowest Gibbs free energy (see below), as ϕ/ϕ_0 is changed from 0.428 to 0.5. The extended core diameter $(1-\alpha)\pi R$ changes from zero for $\phi/\phi_0 < 0.428$ ($\alpha = 1$) to about $0.2\pi R$ at $\phi/\phi_0 = 0.5$ ($\alpha = 0.8^-$). The flux at which the transition to the vortex with an extended core occurs is indicated in Fig. 1 by the curve v. In the region enclosed by curves v and w only the extended vortex core solution is possible, while for R/ξ values above the v and w curves, the even and the extended vortex core solutions are possible.

The normalized Gibbs free-energy difference between the normal and superconducting states is

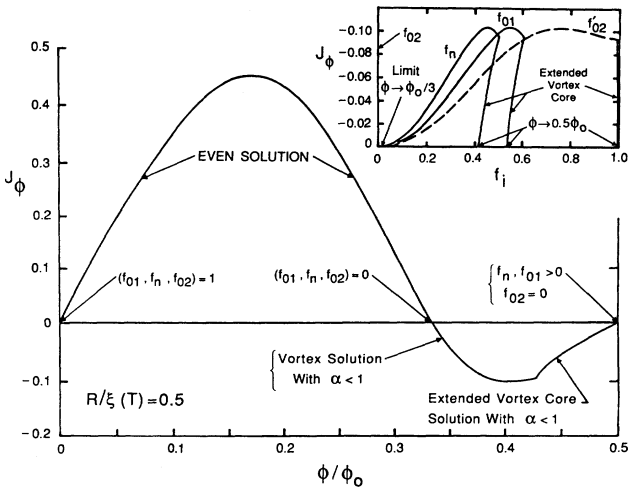

FIG. 3. Normalized persistent current density J_ϕ as a function of magnetic flux ϕ for $R/\xi(T)=0.5$ for the even and odd (vortex) solutions including the extended vortex core solution. The inset shows the corresponding moduli of the order parameters for the two vortex solutions.

$$\Delta G = \int dv[\,\mathbf{A}\cdot\mathbf{J} - \tfrac{1}{2}f^4(x)]\,, \tag{7}$$

where the integral extends over the volume of the bridge circuit. Assuming uniform normalized cross-sectional area S for all branches, the first term on the right-hand side, which can also be written $\frac{1}{2}LJ^2S^2$, is proportional to S^2, while the second term is proportional to S, where L is the normalized self-inductance of the ring. Since distances are normalized by $\xi(T)$, the self-field term is of higher order for a thin filament and may be neglected to first approximation. In particular, if we calculate ΔG at $\phi = 0.5\phi_0$, where $J_\phi = 0$, the self-field term is zero.

Figure 4 shows ΔG as a function of $R/\xi(T)$ for

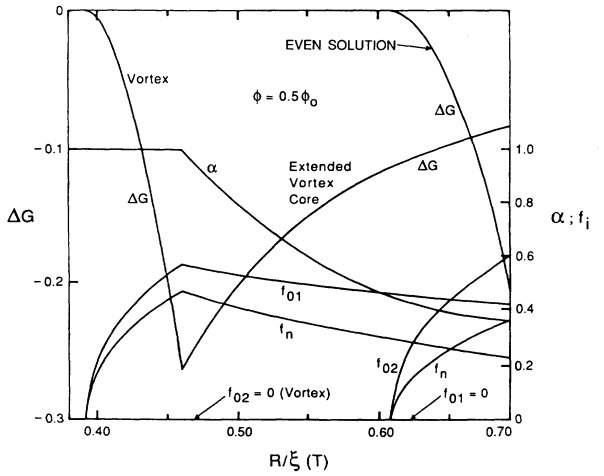

FIG. 4. Normalized Gibbs free-energy differences as a function of $R/\xi(T)$ for $\phi = 0.5\phi_0$ for the odd (vortex) and even solutions. The energy is normalized by $H_c^2(T)S\xi(T)/8\pi$, where H_c is the thermodynamic critical field and S the cross-sectional area of the wires. Also shown are the corresponding moduli of the extremal and nodal order parameters and the core scaling parameter α. For detail see text.

$\phi=0.5\phi_0$ for the conventional vortex, the extended core vortex, and the even solution. The phase transition between the conventional and extended core vortex is first order. For $R/\xi(T)\gtrsim 0.667$, the even solution is of lower energy. Shown also is the scaling factor α of the extended core diameter $(1-\alpha)\pi R$ which corresponds to the lowest Gibbs free energy at a fixed value of R/ξ. Furthermore, f_{01}, f_n, and f_{02} are shown for the odd and even solutions. For the even solution, $f_{01}=0$, which is consistent with $J_\phi=0$ at $\phi=0.5\phi_0$. The singularities in branches 1 and 3 give rise to a phase flip $\Delta\theta=\pm\pi$ in each branch. Perturbation and variational approaches have been also developed and applied to microcircuits near the SOPT such as the bridge circuit and excellent agreement with the exact results is found.[5]

In conclusion, the magnetic properties of our bridge circuit were analyzed using the nonlinear GL theory. There exist two different phase boundaries with distinctly different spatial arrangements of the MOP's. The even solution leads to a maximum MOP on the center branch and to minima on the other branches, while for the odd solution the reverse happens, except that the minimum of the MOP in the center branch is zero, where the phase of the complex order parameter flips by $\pm\pi$. It is interesting to note that the even solution resembles the Meissner state of a bulk superconductor while the counterpart of the odd solution is the surface sheath or the giant vortex state[7] on a cylinder. J_ϕ reverses direction when changing ϕ through $\phi=0$ (and $\phi=\phi_0$), through $\phi=\phi_0/2$, and when leaving and entering the superconducting regions via a normal region, thus reversing the magnetic moment of the circuit. The vortex (odd) solution divides into two domains which are separated by a first-order phase-transition boundary. In one domain, at higher temperatures, a conventional vortex exists while, at lower temperatures, a vortex with an extended vortex core takes over. The extended vortex core should occur in micronetworks, where the current paths are fixed by the geometry, as the distances between the nodes become larger (or at lower temperatures for fixed nodal distance). This is a consequence of satisfying the nodal conditions and the magnetic flux constraint. Recent investigations on the ladder circuit, at one-half flux quantum per unit cell, have found evidence for a normal "core region" at lower temperatures in the middle of every second transverse branch, similar to the above result.[8]

This work was supported in part by National Science Foundation Grant No. INT-8803025. Enlightening discussions with A. López, J. I. Castro, F. de la Cruz, and S. B. Haley are acknowledged.

[1]H. J. Fink and V. Grünfeld, Phys. Rev. B **31**, 600 (1985).
[2]S. Alexander, Phys. Rev. B **27**, 1541 (1983); P. G. de Gennes, C. R. Acad. Sci. Ser. II **292**, 279 (1981).
[3]H. J. Fink, A. López, and R. Maynard, Phys. Rev. B **26**, 5237 (1982).
[4]H. J. Fink and S. B. Haley, Phys. Rev. B **43**, 10 151 (1991).
[5]J. I. Castro, Ph.D. thesis, Universidad Nacional de Cuyo, 1991; J. I. Castro and A. López (unpublished).
[6]H. J. Fink, A. López, and D. Rodrigues, Jpn. J. Appl. Phys. **26**, 1465 (1987).
[7]O. Buisson, P. Gandit, R. Rammal, Y. Y. Wang, and B. Pannetier, Phys. Lett. A **150**, 36 (1990).
[8]H. J. Fink (unpublished).